JOURNAL OF SOLID STATE CHEMISTRY 118, 28–32 (1995)

Synthesis and Characterization of New Quasi-One-Dimensional Mn(II) Hydroxynitrates $(Mn_xZn_{1-x})(OH)(NO_3)H_2O$ (x = 0.53, 1.00)

S. Rouba, P. Rabu,[1] and M. Drillon

IPCMS, UMR046 (CNRS-ULP-EHICS), Groupe des Materiaux Inorganiques, 23 rue du Loess, BP 20/CR, 67037 Strasbourg Cedex, France

Received August 2, 1994; in revised form January 3, 1995; accepted January 10, 1995

The reaction between an aqueous solution of $Mn(NO_3)_2$ and MnO or ZnO gives a white-beige powder of $(Mn_xZn_{1-x})(OH)(NO_3)(H_2O)$ with $x = 1.0$ or $x = 0.53$, respectively. These new manganese(II)-based hydroxynitrates are isostructural with $Zn(OH)(NO_3)(H_2O)$ and crystallize in the monoclinic system, space group $P2_1/c$, with $a = 18.070(2)$ Å, $b = 3.3226(5)$ Å, $c = 14.362(2)$ Å, and $\beta = 114.960(6)°$ for $(Mn_{0.53}Zn_{0.47})(OH)(NO_3)(H_2O)$ and $a = 18.154(2)$ Å, $b = 3.3721(4)$ Å, $c = 14.456(1)$ Å, and $\beta = 114.934(6)°$ for $Mn(OH)(NO_3)(H_2O)$. The manganese(II) atoms are octahedrally coordinated within zigzag double chains running along the b direction. Magnetic measurements from room temperature down to 4.2 K show a quasi-one-dimensional behavior of this special array of classical $S = 5/2$ spins.

INTRODUCTION

The hydroxynitrates of divalent cations, such as Zn(II), Ni(II), Cd(II), and Cu(II), have been widely studied both from a structural and a thermal point of view ((1,2) for example). Thus it was shown that they are good precursors for preparing transition metal oxides, which could be of great interest for catalysis. Indeed, the suitability of hydroxynitrates such as $M_xM'_{1-x}(OH)_y(NO_3)_z \cdot pH_2O$ (M,M' = Cu, Mg, Ni, Zn, Co) for use as precursors of spinel mixed oxides has been demonstrated (3).

Several routes have been reported for the synthesis of transition metal hydroxynitrates. Most consist of the thermal decomposition of hydrated metal nitrate or of the reaction of aqueous nitrate solution with an alkaline agent (KOH, K_2CO_3, or urea, for example). On the other hand, $Cu_2(OH)_3(NO_3)$ (2) was obtained by reacting the metal(II) oxide CuO with concentrated metal nitrate aqueous solution of $Cu(NO_3)_2 \cdot 6H_2O$. In a very recent paper, Meyn *et al.* (4) have generalized this method for the mixed hydroxynitrates $(M,M')(OH)_3(NO_3)$ (M = Zn, Cu, Ni; M' = Co, Ni, Cu).

Further, the low-dimensional character of their magnetic properties has been evidenced for cobalt(II) derivatives (5,6). Angelov *et al.* (5) have shown for the first time that $Co(OH)(NO_3)H_2O$ is a good example of quasi-isolated zigzag double chains of Co(II) ions, the magnetic behavior of which is described on the basis of two competing nearest neighbor interactions. Theoretical studies in the Ising or Heisenberg limits (5–7) have evidenced the occurrence of a frustrated state when intrachain interaction is antiferromagnetic, whatever the sign of interchain interaction.

The present paper reports the synthesis, structural characterization, and magnetic properties of the first manganese-based hydroxynitrates.

EXPERIMENTAL

Metal oxides MO (M = Mn, Zn) are used as the hydrolysis agent in saturated manganese nitrate aqueous solution. The reaction takes place under argon at ambient temperature with a molar ratio $MO/Mn(NO_3)_2$ ranging between 5 and 10. In the first step, mixed Zn/Mn hydroxynitrates were prepared from $ZnO/Mn(NO_3)_2$ mixtures in order to test the suitability of the manganese derivative. Then, a pure Mn compound was prepared. For this purpose, the starting green-colored oxide, MnO, was synthesized by decomposition of manganese(II) oxalate under hydrogen gas flow at 1000°C for 4 hr. The title compounds corresponding to $x = 1.0$ and 0.53 are denoted hereafter as compounds I and II.

Compound I was synthesized after 15 days of hydrolysis with manganese oxide. The reaction product was washed with alcohol and filtered. Compound II was obtained after a preliminary 6-day hydrolysis with ZnO. XRD analysis suggests the presence of several types of hydroxynitrates. By mixing with a fresh manganese nitrate solution, compound II is obtained, after 6 days, as a single-phase product.

The metal content of the compounds was determined from atomic emission measurements or X-ray microanalysis. Differential thermal (DTA) and thermogravimetric (TGA, DTG) analyses were performed using a Setaram TGDTA-92 thermobalance. Powder X-ray diffraction

[1] To whom correspondence should be addressed.

0022-4596/95 $12.00

(XRD) characterizations were carried out at room temperature using a Siemens D500 diffractometer (Cu$K\alpha$ radiation) equipped with a secondary beam graphite monochromator. The program NBSAIDS83 (8) was used for indexing the patterns and refinement of cell parameters. X-ray thermodiffractometry was performed with a high-temperature Guinier camera (Enraf-Nonius) in the range 20–600°C. Magnetic susceptibility and magnetization data were recorded from powder samples by using a Faraday-type fully automated magnetic apparatus (Manics) in the range 4–300 K.

TABLE 1

Crystallographic Cell Parameters and e.s.d.'s, Effective Magnetic Moment and Curie–Weiss Temperature for $(Mn_xZn_{1-x})(OH)(NO_3)H_2O$ with Several Stoichiometries x

x	9(9)	0.53	1.00
a (Å)	17.951(3)	18.070(2)	18.154(2)
b (Å)	3.2600(2)	3.3226(5)	3.3721(4)
c (Å)	14.272(2)	14.362(2)	14.456(1)
β (Å)	114.91(1)	114.960(6)	114.934(6)
V (Å^3)	757.5	781.75	802.4
Z	8	8	8
$\mu_{eff}(\mu_B/Mn)^a$	—	5.7	5.8
θ (K)	—	−21.8	−51.8

[a] The relation with the Curie constant is $C = N\mu_{eff}^2\mu_B^2/3k_B$.

RESULTS

Structural and Thermal Analysis

The XRD patterns of the title compounds exhibit all the same features and display the same characteristics as $Zn(OH)(NO_3)H_2O$ (9) (Fig. 1). The patterns are indexed from monoclinic symmetry (space group $P2_1/c$) and the refined cell parameters are listed in Table 1, with those of the pure zinc derivative (as given by Eriksson *et al.* (9)). The observation of these values shows a notable and quasi-linear enhancement of the cell dimensions with increasing manganese content. A Rietveld profile analysis of the diffraction data has been attempted for $Mn(OH)(NO_3)H_2O$. The program Rietan (10) was carried out using the $Zn(OH)(NO_3)H_2O$ crystallographic data (9) as the starting structure hypothesis. The position parameters of Mn, O (for oxygen, OH groups, or water molecules), and N atoms were refined with an overall temperature factor. The result of the refinements for compound I is illustrated in Fig. 1. The final agreement factors are Rwp = 18.92%, Rp = 13.90%, Re = 11.57% (conventional Rietveld factors), Ri = 6.10%, and Rf = 4.95%. The refined mean Mn–O distances are 2.30 and 2.22 Å for the two sites in agreement with Mn(II) atoms in octahedral coordination with oxygen (11).

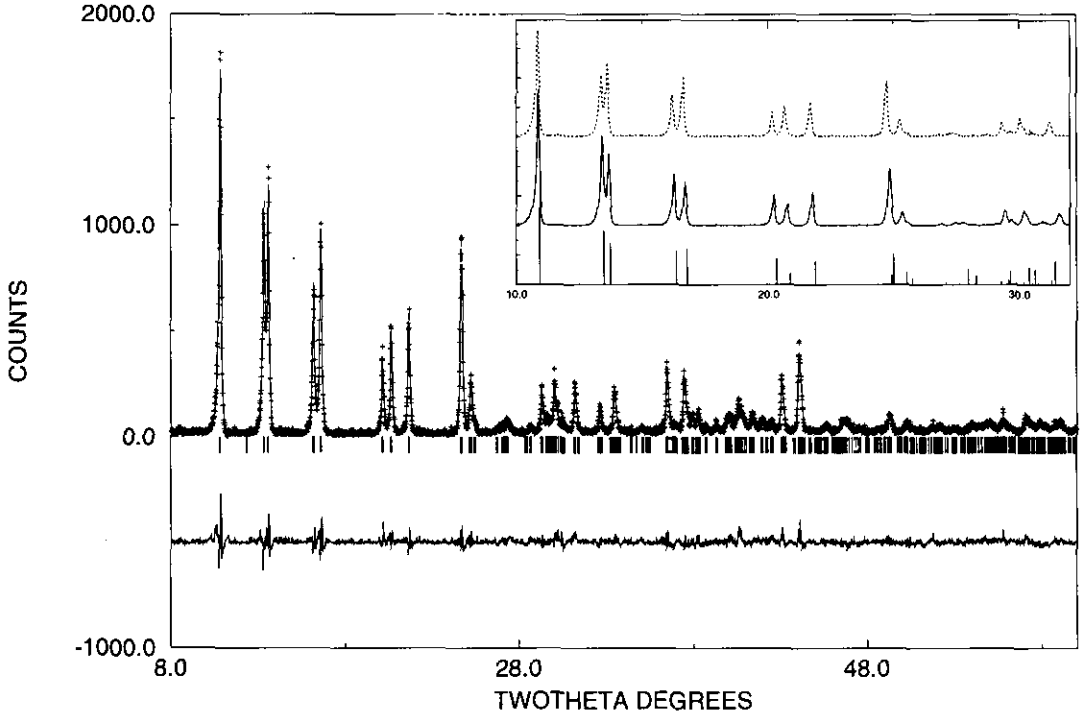

FIG. 1. Upper part shows the experimental (crosses) and refined (full line) patterns with calculated peak positions indicated below; the lower curve shows the difference ($Y_{exp} - Y_{calc}$) for $Mn(OH)(NO_3)H_2O$. Inset: comparison of the characteristic part of the patterns of $(Mn_xZn_{1-x})(OH)(NO_3)H_2O$ compounds for $x = 0$. (vertical bars), $x = 0.53$ (full line), and $x = 1.0$ (dashed line). The height of the bars corresponds to the calculated intensity deduced from the refined parameters given in (9).

The thermal decomposition of I and II has been investigated in air at temperatures from 20 to 630°C at a heating rate of 0.33°C/min. Endothermic decomposition of I occurs in the range 90–110°C, followed by a gradual weight loss up to 270°C, and then a first plateau is observed in the TG curve (Fig. 2a). High-temperature Guinier experiments show the formation of MnO_2, γ-Mn_2O_3, and Mn_2O_3 (bixbyite). Above 480°C, for which a last weight loss occurs, only Mn_2O_3 diffraction lines are observed. The final weight loss (43% in mass) fits well with the transformation of $Mn(OH)(NO_3)H_2O$ into Mn_2O_3.

In the case of the mixed derivative II (Fig. 2b), the thermal behavior is quite similar. The decomposition occurs in the range of 90–110°C, giving an intermediate product whose XRD pattern may be indexed with an orthorhombic unit cell, a = 3.24 Å, b = 5.617 Å, and c = 6.94 Å. A slight shoulder observed in the endothermic decomposition peak (ATD) may be the signature of the formation of this intermediate product. At higher temperatures, a mixture of $ZnMnO_3$, Zn_2MnO_4, and γ-Mn_2O_3 is obtained.

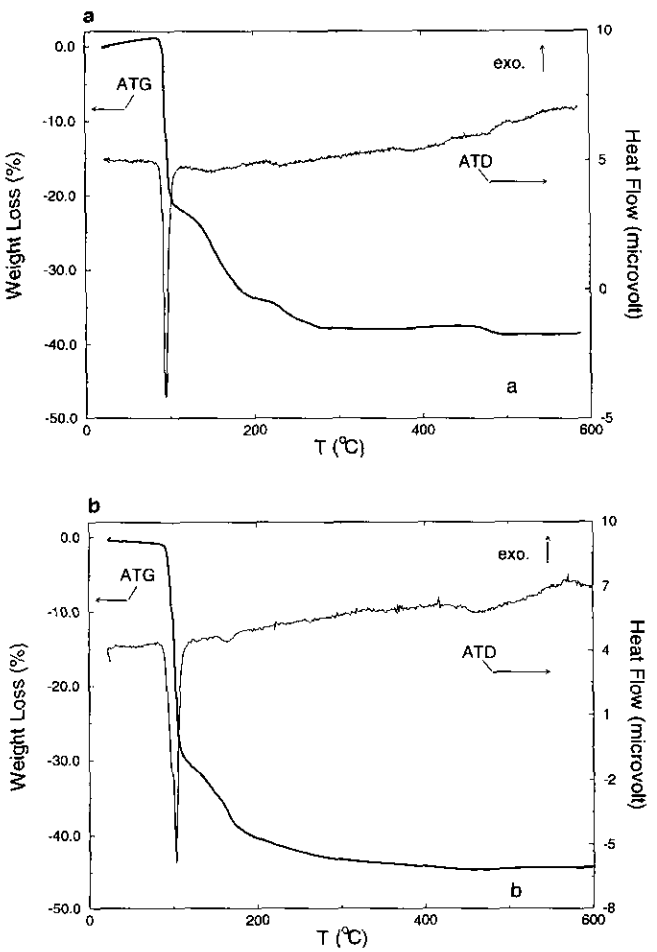

FIG. 2. Thermogravimetric and differential thermal curves in the range 20–650°C for (a) $Mn(OH)(NO_3)H_2O$ and (b) $(Mn_{0.53}Zn_{0.47})(OH)(NO_3)H_2O$. Arrows indicate the corresponding scale axis for ATG and ATD; for the latter, the exothermal variation is specified.

Magnetic Measurements

The temperature-dependent magnetic susceptibility (recorded at 1.3 T) is plotted in Fig. 3. The Curie temperatures, θ, and effective magnetic moments, μ_{eff}, deduced from the high-temperature data are given in Table 1. The μ_{eff} values agree with the presence of Mn(II) (μ_{eff} = 5.9 μ_B/mole (12)) according to the different stoichiometries. The susceptibility of pure manganese compound I exhibits a broad maximum at 28.0 ± 0.5 K indicating that predominant antiferromagnetic interactions take place. It can be noted that the low-temperature variations of the magnetic susceptibility differ for compounds I and II; the latter shows weaker antiferromagnetic coupling.

DISCUSSION

The thermal decomposition scheme in air appears somewhat complex, especially concerning compound II. The presence of an intermediate product at the decomposition step suggests the existence of other manganese(II) hydroxynitrates. Indeed, the hexagonal phase obtained for the mixed derivative II seems very similar to the other two-dimensional compounds $M_2(OH)_3(NO_3)$ (M = Ni, Cu, Co) with regards to their cell parameters (4, 6, 13, 14). Another possibility is that this dehydration product corresponds to the formation of a "degenerate" oxyhydroxynitrate prior to the formation of oxide. The latter has been emphasized, for example, for the topotactic decomposition of layered copper hydroxynitrate (2).

XRD data demonstrate the structural isotypy with the parent compounds $M(OH)(NO_3)H_2O$ (M = Zn, Ni, Co). As described for the zinc derivative (9), their structure may be viewed as the stacking of infinite double chains of edge-sharing octahedra $Mn(OH)_{3/3}(NO_3)_{1/1}(H_2O)_{2/2}$ running along the b axis (Fig. 4a). Within elementary chains, the Mn(II) octahedra are linked by one oxygen (of a water molecule) and one hydroxyl ion, while these chains are connected to each other through hydroxyl ions only. Finally, nitrate groups are linked to the other unshared corners and thus maintain the packing of twin chains through hydrogen bonds with water molecules. It should be emphasized that two distinct orientations of the double chains exist in the (a, c) plane.

The presence of separated doublets of diffraction lines in the low 2θ range of the XRD patterns points out that I and II are isostructural with the model compound $Zn(OH)(NO_3)H_2O$ described above. Note that for other derivatives the diffraction patterns may exhibit single lines instead of doublets, probably due to variations in the chain stacking, as discussed by Petrov *et al.* (15) for $Co(OH)(NO_3)H_2O$. Well-crystallized $Ni(OH)(NO_3)H_2O$

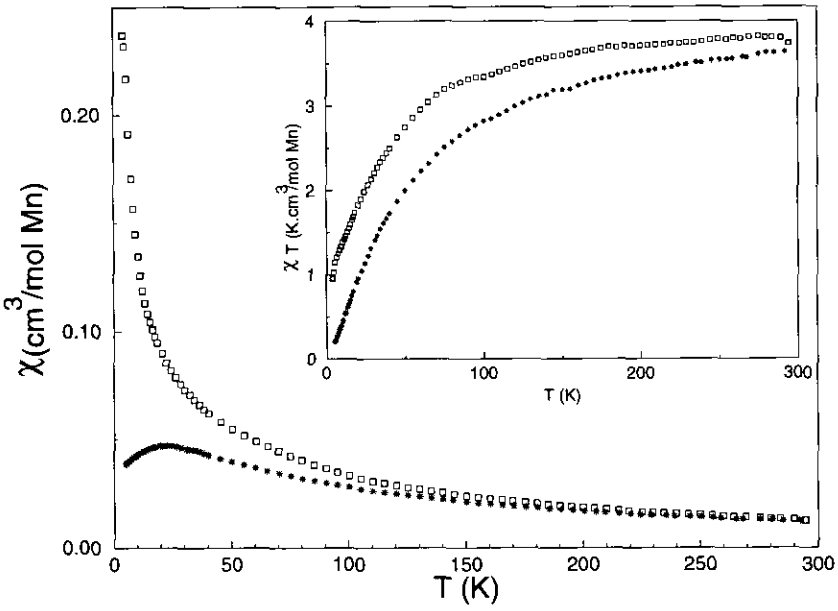

FIG. 3. Variation in the magnetic susceptibility with temperature for $(Mn_xZn_{1-x})(OH)(NO_3)(H_2O)$, with $x = 0.53$ (□) and 1 (*); the χT product is plotted in the inset.

(with separated doublets) is obtained only after hydrothermal treatment (1). The goodness of the Rietveld profile refinement is not very high. Indeed, some difficulties appeared when the atomic parameters were refined, especially for the *y* coordinates. As discussed in (9), this is linked to the presence of a very short *b* axis. Moreover, in the present work, the accuracy of the intensities is lowered due to the use of nonseparated $\alpha 1$-$\alpha 2$ radiations, the preferential orientation effect (last parameter fitted), and the slightly hygroscopic character of the powder sample. The latter is also a limiting factor in order to perform data collection with long counting time. Note that similar problems were encountered in (9), though of less severity (essentially) because of a better resolution of the experimental record (strictly monochromatic Cu radiation was used). Despite these drawbacks, it can be assumed that the powder structure refinement of $Mn(OH)(NO_3)H_2O$ confirms the structural isotypy with the zinc derivative.

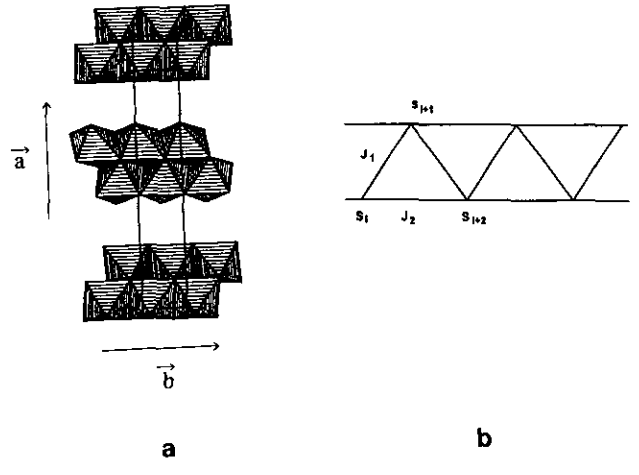

FIG. 4. Structure of $Mn(OH)(NO_3)H_2O$: (a) stacking of the octahedra surrounding the manganese atoms and (b) sketch of the exchange pathways corresponding to first neighbor interactions J_1, between the chains, and J_2, along the chains of $S = 5/2$ spins.

Finally, as expected from the metal–oxygen bond lengths for octahedral Zn(II) and Mn(II) (2.14 and 2.22 Å, respectively (11)), a regular (quasi-linear) increase in the size of the unit cell with manganese content is observed in agreement with the existence of a solid solution $(Mn_xZn_{1-x})(OH)(NO_3)H_2O$ throughout the whole range $0 \leq x \leq 1$.

From magnetic point of view, the $\chi T = f(T)$ variation for $Mn(OH)(NO_3)H_2O$ shows clearly the predominance of antiferromagnetic exchange interaction between $S = 5/2$ spins along the double chains of Mn(II). The broad maximum of the susceptibility confirms the low-dimensional (quasi-1*d*) character of this compound. As discussed in preceding works (5, 7), it may be viewed indeed as the stacking of double chains of $S = 5/2$ spins, with two competing interactions, J_1 between the elementary chains (zigzag pathway), and J_2 along these chains (Fig. 4b). The lack of a χT maximum for compound II may be explained by the introduction of zinc atoms. Indeed, the presence of diamagnetic cations along the chains induces a break in the exchange pathways. Then the material reduces to a distribution of quasi-linear finite-sized clusters. The presence of a plateau at 5 K in the χT curve for compound II may be directly related to isolated manga-

nese cations. The continuous divergence of the susceptibility upon cooling suggests that the interactions between the double chains are very small, and chiefly that the maximum observed for the pure manganese compound is due to intrachain interactions.

CONCLUDING REMARKS

The use of manganese oxide as a hydrolysis agent in nitrate solution has allowed the synthesis of the first manganese-based hydroxynitrates. The preparation of mixed samples with zinc suggests the existence of a complete (well-crystallized) solid solution $(Mn_xZn_{1-x})(OH)(NO_3)H_2O$ $(0 \leq x \leq 1)$. These materials may constitute interesting precursors of fine manganese-based oxides at relatively low temperature. Temperature-resolved X-ray diffractometry studies must be detailed in order to specify their complex thermal decomposition. Supplementary magnetic measurements, such as magnetization versus field, low field susceptibility, neutron diffraction, and temperature-dependent specific heat, are in progress. A convenient theoretical model for classical isotropic spin in a zigzag double chain is currently being developed for a good understanding of the competition between exchange interactions in this unusual low-dimensional magnetic system.

ACKNOWLEDGMENTS

We thank Dr. Najmi and collaborators (CRITT materiaux, Schiltigheim, France) for X-ray measurements and the European community (European Network for Molecular Magnetism) for their support.

REFERENCES

1. M. Louër, and D. Grandjean, *Acta Crystallogr. Sect. B* **29,** 1696 (1973); M. Louër, D. Louër, D. Grandjean, and D. Weigel, *Acta Crystallogr. Sect. B* **29,** 1707 (1973).
2. J. P. Auffrédic, D. Louër, and M. Louër, *J. Therm. Anal.* **16,** 329 (1979).
3. L. Markov, K. Petrov, and V. Petkov, *Thermochim. Acta.* **106,** 283 (1986); K. Petrov and L. Markov, *J. Mater. Sci.* **29,** 1211 (1985); K. Petrov, L. Markov, R. Ioncheva, and P. Rachev, *J. Mater. Sci.* **23,** 181 (1988); K. Petrov, K. Krezhov, and P. Konstantinov, *J. Phys. Chem. Solids* **50,** 577 (1989); L. Markov, K. Petrov, and A. Lyubchova, *Solid State Ionics* **39,** 187 (1990).
4. M. Meyn, K. Beneke, and G. Lagaly, *Inorg. Chem.* **32,** 1209 (1993).
5. S. Angelov, M. Drillon, E. Zecheva, R. Stoyanova, M. Belaiche, A. Derory, and A. Herr, *Inorg. Chem.* **31,** 1514 (1992).
6. P. Rabu, S. Angelov, P. Legoll, M. Belaiche, and M. Drillon, *Inorg. Chem.* **32,** 2463 (1993).
7. M. Drillon, P. Rabu, and P. Legoll, *in* "Trends in Inorganic Chemistry," Vol. 3, p. 581. Research Trends Publishers, India, 1993.
8. A. D. Mighell, C. R. Hubbard, and J. K. Stalik, "Technical Note 1141," National Bureau of Standards, Washington, DC, 1981; NBS*AIDS83 is an expanded version of NBS*AIDS80.
9. L. Eriksson, D. Louër, and P. E. Werner, *J. Solid State Chem.* **81,** 9 (1989).
10. RIETAN: Fortran 177 software package for Rietveld analysis, F. Izumi, *Nippon Kessho Gakkaishi* **27,** 23 (1985); *Rigaku J.* **6,** 1 and 10 (1989).
11. P. Poix, *C. R. Acad. Sci. Paris* **268,** 1139 (1969).
12. R. L. Carlin, *in* "MagnetoChemistry." Springer-Verlag, Berlin/Heidelberg (1986).
13. P. Gallezot and M. Prettre, *Bull. Soc. Chim. Fr.* **2,** 407(1969).
14. H. Heffenberger, *Z. Kristallog.* **165,** 127 (1983).
15. K. Petrov, N. Zotov, and O. Garcia-Martinez, *J. Solid State Chem.* **101,** 145 (1992).